Vol 17 No 9, September 2008
1674-1056/2008/17(09)/3322-07

Chinese Physics B

© 2008 Chin. Phys. Soc.
and IOP Publishing Ltd

Isotope effect in collision between helium atom and hydrogen bromide molecule*

Yu Chun-Ri(余春日)[a)†], Cheng Xin-Lu(程新路)[b)], and Yang Xiang-Dong(杨向东)[b)‡]

[a)] *School of Physics & Electric Engineering, Anqing Teachers College, Anqing* 246133, *China*
[b)] *Institute of Atomic and Molecular Physics, Sichuan University, Chengdu* 610065, *China*

(Received 23 November 2007; revised manuscript received 21 April 2008)

The anisotropic potential developed in our previous research and the close-coupling method are applied to the HBr–^{3}He (^{4}He, ^{5}He, ^{6}He, ^{7}He) system, and the partial cross sections (PCSs) at the incident energy of 60 meV are calculated. Based on the calculations, the influences of the isotope helium atom on PCSs are discussed in detail. The results show that the excitation PCSs converge faster than the elastic PCSs for the collision energy and the systems considered here. Also the excitation PCSs converge more rapidly for the high-excited states. The tail effect is present only in elastic scattering and low-excited states but not in high-excited states. With the increase of reduced mass of the collision system, the converging speed of the elastic and excitation PCSs slows down, and the tail effect goes up.

Keywords: isotope effect, partial cross section, anisotropic potential, HBr–He collision
PACC: 3440, 3450

1. Introduction

The inelastic scattering of an atom by a diatomic molecule has been the subject of numerous experimental and theoretical studies. It plays a significant role in such practical processes as gas phase relaxation, gas phase reaction, energy transfer in chemical laser, resonance fluorescence, thermal scattering in mixture gases, and cooling process in planetary space.[1−5] The van der Waals rare gas complexes Rg–HX (X = F, Cl)[6−8] have often been considered as model systems for investigating both weakly neutral non-covalent interactions and collision dynamics. Recently, interest has been focused both theoretically and experimentally on the structure and molecular dynamics of the third and fourth row hydrogen halides, HBr and HI, and their interactions with the rare gas atoms Rg = He, Ne, Ar. Held *et al*[9] presented the exponential-spline–Morse-spline–van der Waals (ESMSV) interaction potential for He–HBr system. Sun *et al*[10] found that the ESMSV potential is a discontinuous function because of having two interrupted regions, and a Morse function is added in order to describe the interaction potential in the interrupted regions. However, the ESMSV potential cannot be applied to inelastic scattering because of its spherical symmetry. In 2002, Zhang *et al*[11] calculated the interaction energies for a series of linear and nonlinear geometries in the rigid He–HBr system (the distance between Br and H is fixed at its equilibrium value) using the augmented correlation-consistent polarized quadruple zeta basis set aug-cc-pVQZ at the theoretical level of the coupled cluster singles and doubles including connected triple excitations [CCSD (T)]; and the counterpoise method of Boys and Bernardi[12] was used to eliminate the basis set superposition error (BSSE). Based on the Zhang's data, we have obtained an anisotropic potential[13] for the He–HBr system. So far as we know, little of the isotope effect in collision between helium atom and hydrogen bromide molecule has been reported.

The aim of this paper is to obtain the effects of the isotope helium atoms on the partial cross sections (PCSs). This paper is organized as follows. In the next section, we briefly review the close-coupling approach used in our calculation, the anisotropic potential established in our previous research for the He–HBr system is then presented. Subsequently, the calculated results for the elastic and inelastic PCSs and the comparison with previous theoretical findings are reported. Conclusions are given in the last section.

*Project supported by the Natural Science Foundation of Anhui Education Bureau of China and the National Natural Science Foundation of China (Grant Nos 10676025 and 10574096).
†E-mail: cryu2@126.com
‡Corresponding author. E-mail: xdyang@scu.edu.cn

2. Theoretical calculations

2.1. The close-coupling method

The Hamiltonian of the scattering system between an atom and a diatomic molecule can be expressed as[14]

$$H = -\frac{\hbar^2}{2\mu_{\mathrm{A,BC}}}\nabla_R^2 - \frac{\hbar^2}{2\mu_{\mathrm{BC}}}\nabla_r^2 + V(\hat{\boldsymbol{R}}, \hat{\boldsymbol{r}}, \cos\theta), \quad (1)$$

where $\mu_{\mathrm{A,BC}}$ and μ_{BC} are the total reduced mass of the scattering system and the reduced mass of the diatomic molecule respectively, and $\cos\theta = \hat{\boldsymbol{R}}\cdot\hat{\boldsymbol{r}}$. The total wavefunction of the system has the following form

$$\psi_\alpha(\boldsymbol{R}, \boldsymbol{r}) = \frac{1}{K_{n_\alpha j_\alpha} R} \sum_{n_\gamma j_\gamma l_r J} g^J_{n_r j_r l_r, n_a j_a M_a}(R) \times \phi_{n_r j_r}(r) Y^{l_r j_r}_{J M_\alpha}(\hat{\boldsymbol{R}}, \hat{\boldsymbol{r}}), \quad (2)$$

where $g(R)$ is the radial wavefunction of the relative motion between the atom and diatom, $\phi\ (r)$ is the radial part of the ro-vibrational wavefunction for the diatomic molecule, α is the incident channel and γ is the other possible channel, n is the vibrational quantum number, J is the quantum number of total angular momentum of the system, and l_γ and j_γ are the orbital quantum number of the incident atom and the rotational quantum number of the molecule in γ channel, respectively. The total wavefunction $\psi_\alpha(\boldsymbol{R}, \boldsymbol{r})$ is given by the solution of the Schrödinger equation

$$(H - E)\psi_\alpha(\boldsymbol{R}, \boldsymbol{r}) = 0. \quad (3)$$

Substituting Eqs.(1) and (2) into the corresponding parts of Eq.(3), we have

$$\left(\frac{\mathrm{d}^2}{\mathrm{d}R^2} - \frac{l_\beta(l_\beta+1)}{R^2} + k^2_{n_\beta j_\beta}\right) g^J_{n_\beta j_\beta l_\beta, n_a j_a M_a}(R) = \frac{2\mu_{\mathrm{A,BC}}}{\hbar^2} \sum_{n_r j_r l_r} V^J_{n_\beta j_\beta l_\beta, n_\gamma j_\gamma l_\gamma}(R) \times g^J_{n_\beta j_\beta l_\beta, n_a j_a M_a}(R). \quad (4)$$

Equation (4) is the close-coupling equation in atom–diatomic collisions.

2.2. The anisotropic potential for He–HBr

Ab initio calculation of the interaction energy between ^{4}He and HBr has been performed by Zhang *et al*[11] for intermolecular distance in the interval from 0.36 nm to 0.46 nm, and 11 angles in the range from 0° to 180°. The conventional Jacobi coordinate system (R, r, θ) is used in all calculations, where r is the bond length of HBr (fixed at 0.1421 nm, according to the calculation at the CCSD(T)/aug-cc-pVQZ theory level), R is the separation from the centre of mass of HBr molecule to the He atom, and θ is the angle describing the orientation of the He atom with respect to the HBr bond axis, and 0° corresponds to the collinear He–H–Br geometry. The variation of the potential energy surface (PES) as a function of the He–HBr separation for several relative orientations is shown in Fig.1.

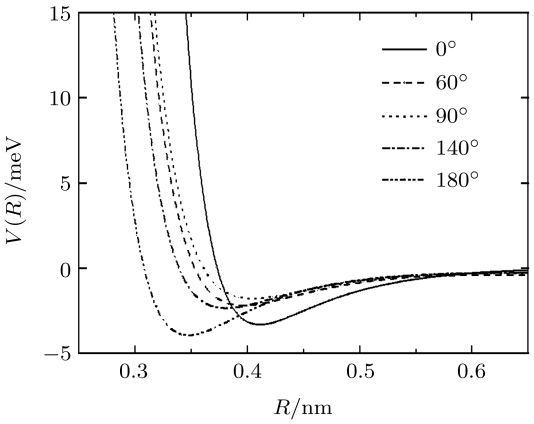


Fig.1. Section of the He–HBr potential energy surface associated with the selected Jacobian angles.

From the PES we can see that the global minimum has an energy of –3.981 meV at $R = 0.347$ nm in the He–Br–H linear configuration ($\theta = 180°$), a secondary minimum has an energy of –3.351 meV at $R = 0.410$ nm in the He–H–Br linear configuration ($\theta = 0°$), and an intervening saddle point of –1.803 meV at $R = 0.403$ nm in the T-shaped configuration ($\theta = 90°$).

The anisotropic potential is the same for the HBr–^{3}He (^{4}He, ^{5}He, ^{6}He, ^{7}He) systems although the masses of the isotope helium atoms are different. In preparation for a scattering dynamics calculation, the discrete ab initio potential energy points are usually fitted into an analytic expression. We expand the Zhang's PES in Legendre polynomials as

$$V(R, \theta) = \sum_\lambda V_\lambda(R) P_\lambda(\cos\theta), \quad (5)$$

where each radial potential $V_\lambda(R)$ ($\lambda = 0, 1, 2, 3, 4$) can be expressed by employing the Barker potential

function form[15]

$$V_\lambda(R) = \varepsilon\left[\exp(\alpha(1-x))\sum_{n=0}^{3} A_n (x-1)^n - \frac{C_6}{x^6+\delta} - \frac{C_8}{x^8+\delta}\right]. \quad (6)$$

Here, $x = R/R_\mathrm{m}$, R_m is the position of potential well, ε is the depth of potential well, α, A_0, A_1, A_2, A_3, C_6, C_8 and δ are the fitted parameters, which are described in Ref.[13].

Figure 2 shows a comparison between the spherical symmetry terms V_0 resulting from our anisotropic potential and the isotropic ESMSV potential.[9] The well depth of our V_0 is 2.19 meV, which is deeper than that of the ESMSV potential, the latter is 1.90 meV. The well position of our V_0 is located at 0.396 nm, which is smaller than that of the ESMSV potential, the latter is 0.399 nm. Our anisotropic potential is closer to the real interaction of the He–HBr system from a comparison of the differential cross sections (DCSs) calculated based on the two theoretical potentials with the experimental result in the next section.

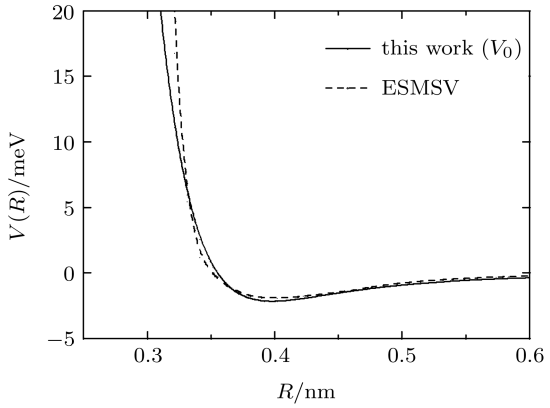


Fig.2. Comparison of our potential with the ESMSV potential.

3. Results and discussion

By solving the close–coupling differential equation, the PCSs for collisions of HBr molecule with ^{3}He (^{4}He, ^{5}He, ^{6}He, ^{7}He) atom at the incident energy of 60 meV are calculated. The rotational basis sets include all the energetically open rotational channels and at least two energetically closed channels. The calculated partial wave number is 110 for each of excitations. We assume that the partial wave is convergent when the PCS reaches $10^{-4}a_0^2$, where a_0 is Born radius.

In order to verify the reliability of our anisotropic potential and close-coupling calculations at lower energy scattering, using our anisotropic potential and the ESMSV, we calculate the total DCSs for collisions of HBr with ^{4}He at the incident energy of 75 meV. The results are compared with the experimental data[9] as shown in Fig.3. It can be seen from Fig.3 that the oscillating positions and amplitudes of the DCSs for our anisotropic potential are in agreement with the experimental data, whereas the DCSs of the ESMSV potential are obviously smaller than the experimental data at the second minimum position and the larger scattering angles. According to the scattering cross section data, our anisotropic potential and the close-coupling calculations of scattering cross sections are reliable.

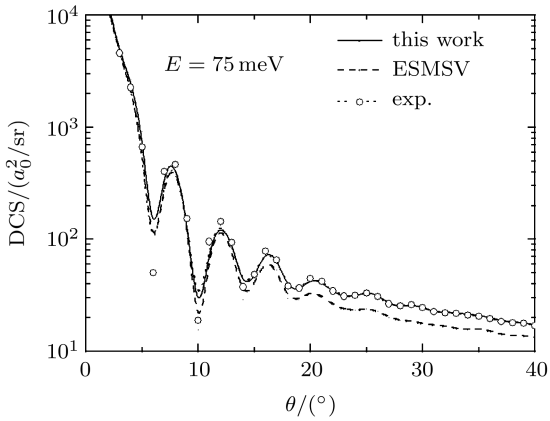


Fig.3. Comparison of the total DCSs of the theoretical potentials with the experimental data.

Figures 4 and 5 show the variations of the elastic and total inelastic PCSs for collisions between HBr molecules and isotope ^{3}He (^{4}He, ^{5}He, ^{6}He, ^{7}He) atoms with the increase of total angular quantum number J at the incident energy of 60 meV. From Fig.4, it can be seen easily that the tendencies of the elastic PCSs varying with J for the different isotope He atoms are similar, which is described as follows: the PCSs keep oscillatory with the increase of quantum number J, at the given incident energy, the oscillating amplitude increases until it finally reaches a maximum, and then tends toward zero rapidly. We can also learn from Fig.4 that there exists an obvious tail effect when the elastic PCSs converge because of quantum effect. Table 1 lists the peak value of the elastic PCS, corresponding partial wave number J, tail maximum value, corresponding partial wave number J', and convergent partial number J_max.

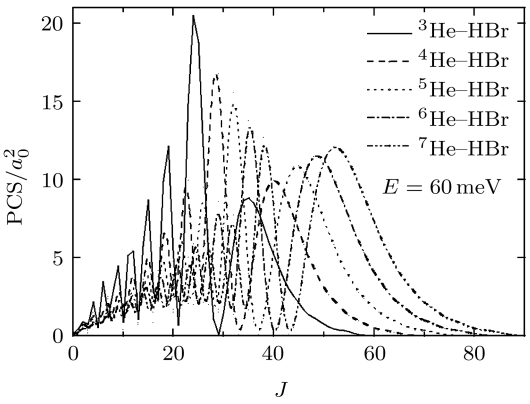


Fig.4. The elastic PCSs for scatterings of isotope He atoms with HBr molecules.

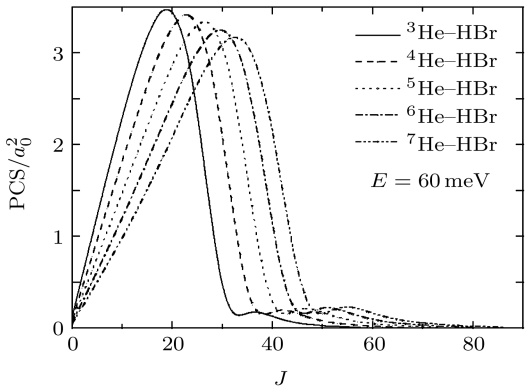


Fig.5. The total inelastic PCSs for scatterings of isotope He atoms with HBr molecules.

Table 1. The peak value of the elastic PCS, corresponding partial wave number J, tail maximum value, corresponding partial wave number J', and convergent partial wave number $J_{\max}$ for collisions of isotope He atoms with HBr molecules.

collision system	peak value/a_0^2	J	tail max. value/a_0^2	J'	$J_{\max}$
^{3}He–HBr	20.5	24	8.82	35	62
^{4}He–HBr	17.2	28	9.95	40	71
^{5}He–HBr	15.6	32	10.9	45	78
^{6}He–HBr	13.8	35	11.5	48	85
^{7}He–HBr	12.7	38	12.1	52	90

From Fig.4 and Table 1, it can be seen clearly that the tail effect becomes stronger and stronger with the increase of the isotope He atom mass. For instance, when the incident particle is ^{3}He atom, the tail maximum value is 8.82 a_0^2 at $J = 35$. When the incident particle is ^{7}He atom, the tail maximum value is 12.1 a_0^2 at $J = 52$. This phenomenon results from a quantum effect. When the angular quantum of the incident particle is large enough, the particle cannot interact with the scattering potential field from the viewpoint of classical scattering, but the particle can still be scattered by the potential field because of quantum effect. At the same collision energy, the larger the mass of the incident helium atom, the more prominent the quantum effect, which results in the stronger tail effect.

From Fig.4 and Table 1, it also can be seen that the variation of elastic PCSs and their converging speed slow down with the increase of the isotope helium atom mass. For example, when the incident atom is ^{3}He, the elastic PCSs reach a peak value of 20.5 a_0^2 at $J = 24$, the converging partial wave number is 62 if the tail effect is considered. When the incident atom is ^{7}He, the elastic PCSs reach a peak value of 12.7 a_0^2 at $J = 38$, the converging partial wave number is 90. This is understandable because, semiclassically, the condition that an incident particle can be elastically scattered in a centre potential field is $l \leq a\sqrt{2\mu E}/\hbar$,[16] where a is the effective interaction radius of the centre potential field, μ denotes the reduced mass, E denotes the collision energy. Here, the molecule is initially in a ground rotational state $j_\alpha = 0$, the total angular momentum J equals the orbital angular momentum l of the incident channel. Therefore, the number $J_{\max}$ corresponding to the converging elastic PCS can be described as

$$J_{\max} = a\sqrt{2\mu E}/\hbar. \tag{7}$$

Obviously, for the given incident energy and the identical scattering potential field (the same effective interaction radius of the field), $J_{\max}$ is in proportion to the square root of μ. With the increase of the reduced mass, the $J_{\max}$ corresponding to the converging elastic PCS gradually shifts towards large value of J.

We can see from Fig.5, with the increase of the isotope helium atom mass, the total inelastic PCS and its converging speed decrease, and yet its tail effect increases. Combining Fig.5 with Fig.4, we can also see that the total inelastic PCS converges faster than that of the elastic PCS. For example, for ^{3}He–HBr system, the converging partial wave of the total inelastic PCS is less than that of the elastic PCS, the former is 59, while the latter is 62 when the tail effect is consid-

ered. For the ^{7}He–HBr system, the converging partial wave of the total inelastic PCS is less than that of the elastic PCS: the former is 89, and the latter is 90.

Figures 6–11 show the variations of the state-to-state excitation PCSs for collisions between HBr molecule and isotope ^{3}He (^{4}He, ^{5}He, ^{6}He, ^{7}He) atom with J at the incident energy of 60 meV. We can see the quantitative variations from the cross sections in Fig.5–11, of the five collision systems, the total inelastic PCSs come mainly from the transitions of $nj >= 00 \rightarrow nj' >= 01, 02$. And there exists a tail effect for the transitions of 00→01, 00→02, but no tail effect for the higher rotational transitions of 00→03, 00→04 and so on. Therefore, it is indicated that the tail effect is present only in lower excited states but not in higher excited states.

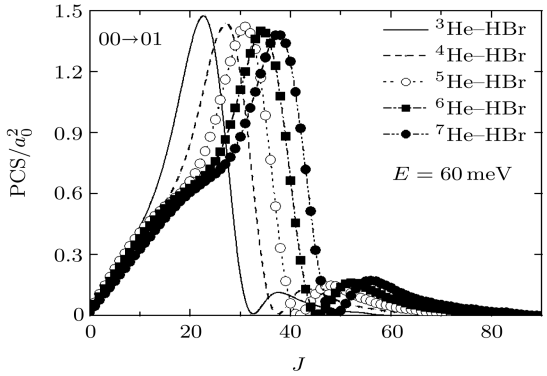


Fig.6. The state-to-state excitation PCS versus J for collisions of isotope He atoms with HBr molecules for excitation 00 → 01.

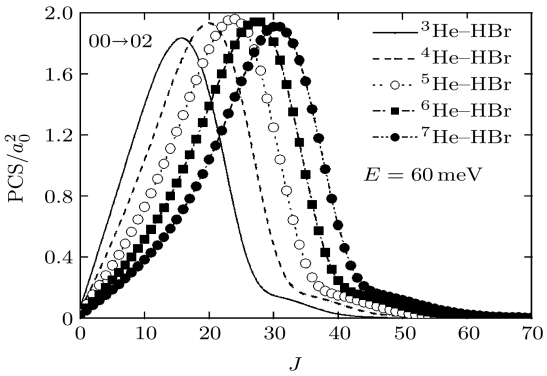


Fig.7. The state-to-state excitation PCS versus J for collisions of isotope He atoms with HBr molecules for excitation 00 → 02.

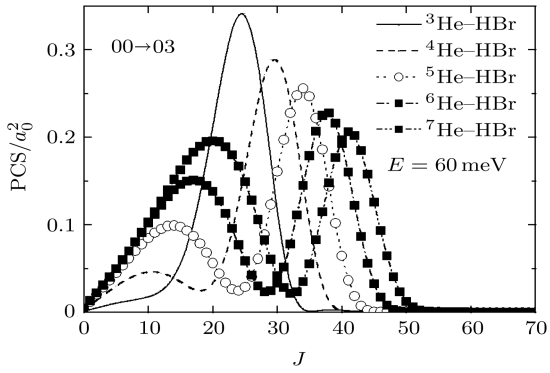


Fig.8. The state-to-state excitation PCS versus J for collisions of isotope He atoms with HBr molecules for excitation 00 → 03.

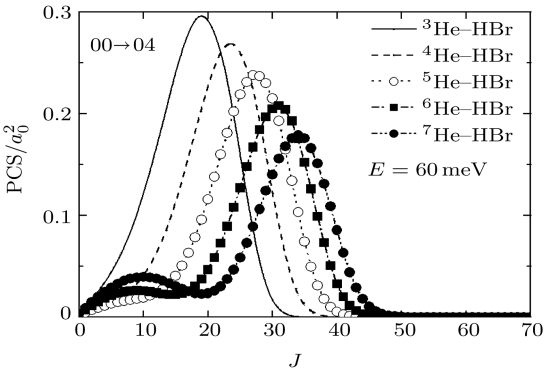


Fig.9. The state-to-state excitation PCS versus J for collisions of isotope He atoms with HBr molecules for excitation 00 → 04.

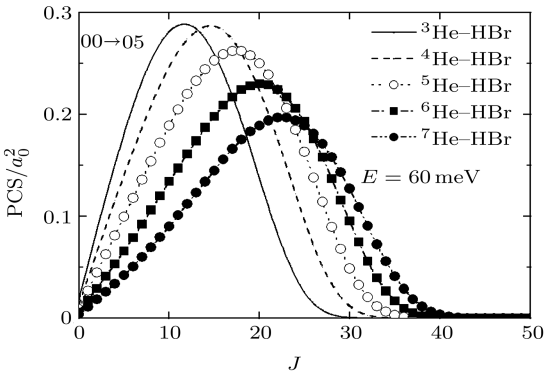


Fig.10. The state-to-state excitation PCS versus J for collisions of isotope He atoms with HBr molecules for excitation 00 → 05.

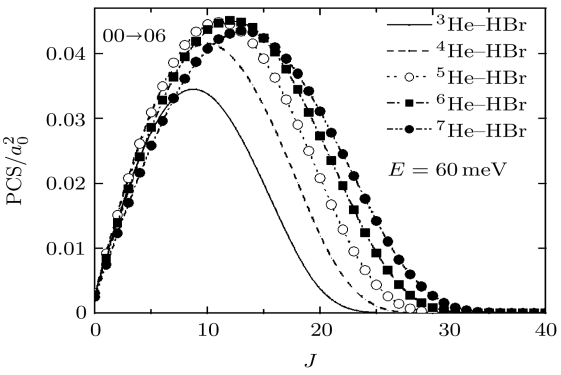


Fig.11. The state-to-state excitation PCS versus J for collisions of isotope He atoms with HBr molecules for excitation 00 → 06.

Table 2 displays the peak value of each state-to-state excitation PCS, corresponding partial wave number J, and the converged partial wave number $J_{\max}$ for the five collision systems. From these figures and tables above, it can be seen that the tendencies of the state-to-state excitation PCS varying with J for the different isotope He atoms are similar, i.e. the higher the excitation state, the more rapidly the excitation PCS converges, and the less the converging partial wave number. For each excitation, with the increase of mass of the isotope helium atom, the converging speed of the state-to-state excitation PCS slows down, and needs more partial waves to converge. For example, corresponding to the excitation of 00 → 01 for the HBr-^{3}He (^{4}He, ^{5}He, ^{6}He, ^{7}He), the converging partial waves are 59 (68, 75, 82 and 88) respectively. For the excitation of 00 → 06, the converging partial waves are 22 (25, 28, 30 and 32) respectively.

From Figs.6–11 and Table 2, it can be seen also that the peak values of the excitation PCSs for the five collision systems are present in the excitation of 00 → 02. Take the ^{3}He–HBr system as an example, the PCSs of 00 → 02 excitation reach the peak value of 1.84 a_0^2 at $J = 16$, and the peak value of 1.91a_0^2 at $J = 30$ for the ^{7}He–HBr. In addition, with the increase of the mass of isotope He atom, the maximum of the PCSs for each excitation of 00 → 01, 03, 04, 05 decreases, whereas for the 00 → 02, 06 excitations, it first increases and then decreases.

Table 2. The peak value of the state-to-state excitation PCS, corresponding partial wave number J, and convergent partial wave number $J_{\max}$ for collisions of isotope He atoms with HBr molecules.

collision system	^{3}He–HBr			^{4}He–HBr			^{5}He–HBr			^{6}He–HBr			^{7}He–HBr		
transition	PCS/a_0^2	J	$J_{\max}$	PCS/a_0^2	J	$J_{\max}$	PCS/a_0^2	J	$J_{\max}$	PCS/a_0^2	J	$J_{\max}$	PCS/a_0^2	J	$J_{\max}$
00→01	1.48	23	59	1.44	27	68	1.42	31	75	1.40	34	82	1.38	37	88
00→02	1.84	16	49	1.94	20	57	1.96	24	63	1.94	27	69	1.91	30	74
00→03	0.342	24	35	0.290	30	40	0.256	34	45	0.228	38	50	0.206	41	54
00→04	0.297	19	33	0.269	23	39	0.238	27	43	0.208	31	46	0.179	34	49
00→05	0.289	12	30	0.287	14	34	0.262	17	37	0.230	20	40	0.197	22	42
00→06	0.0346	9	22	0.0417	10	25	0.0449	11	28	0.0451	12	30	0.0435	13	32

4. Conclusions

Based on the above discussion for HBr–^{3}He (^{4}He, ^{5}He, ^{6}He, ^{7}He) collision systems, the effects of the isotope helium atoms on PCSs at the collision energy of 60 meV have been obtained. We can summarize the results as follows:

(1) For the collision energy and systems considered here, the excitation PCSs converge faster than the elastic PCSs, and the excitation PCSs converge more rapidly for the high-excited states. With increasing reduced mass of the collision system, the converging speeds for the elastic, total inelastic and state-to-state excitation PCSs slow down.

(2) The tail effect exists only in elastic scattering and low-excited states but not in high-excited states; and the larger the reduced mass of the collision system, the stronger the tail effect.

(3) With the increase of reduced mass of the collision system, the elastic and total inelastic PCSs, which come mainly from the transitions of 00 → 01 and 02, decrease.

(4) As far as the collision energy and systems are concerned here, the peak value of the excitation PCS is present in the excitation of 00 → 02. In addition, for each excitation, the maximum of the excitation PCS undergoes a regular change with increasing reduced mass of the collision system.

These results can serve as reference in further scattering experiments and theoretical studies of weakly interacting molecules.

References

[1] Sitlani A and Barton J K 1994 *Biochemistry* **33** 12100

[2] Yang X D 1990 *Sci. Chin.* A **33** 833 (in Chinese)

[3] Feng E Y, Huang W Y, Cui Z F and Zhang W J 2004 *Chem. Phys.* **303** 309

[4] Wang R K, Linghu R F and Yang X D 2007 *Acta Phys. Sin.* **56** 2067 (in Chinese)
[5] Shen G X, Linghu R F, Wang R K and Yang X D 2007 *Chin. Phys.* **16** 3352
[6] Chapman W B, Weida M J and Nesbitt D J 1997 *J. Chem. Phys.* **106** 2248
[7] Yu C R, Huang S Z, Feng E Y, Wang R K, Cheng X L and Yang X D 2006 *Acta Phys. Sin.* **55** 2215 (in Chinese)
[8] Yu C R, Wang R K, Cheng X L and Yang X D 2007 *Acta Phys. Sin.* **56** 2577 (in Chinese)
[9] Held W D, Piper E, Ringer G and Toennies J P 1980 *Chem. Phys. Lett.* **75** 260
[10] Sun G H, Yang X D, Zhu J and Wang C X 2002 *Chin. Phys.* **11** 910
[11] Zhang Y, Shi H Y and Wang W Z 2002 *Acta Chim. Sin.* **60** 1011 (in Chinese)
[12] Boys S F and Bernardi F 1970 *Mol. Phys.* **19** 553
[13] Yu C R, Feng E Y, Wang R K and Yang X D 2006 *Chin. Phys.* **15** 2571
[14] Choi B H and Tang K T 1975 *J. Chem. Phys.* **63** 1775
[15] Boughton C V, Miller R E, Vohralik P F and Watts R O 1986 *Mol. Phys.* **58** 827
[16] Muckerman J T and Truhlar D G 1979 *Atom–Molecule Collision Theory: a Guide for the Experimentalist* (New York: Plenum) p33